

## E/M dips

### Evidence for lipids regularly distributed into hexagonal super-lattices in pyrene-PC/DMPC binary mixtures at specific concentrations

Daxin Tang and Parkson Lee-Gau Chong

Department of Biochemistry, Meharry Medical College, Nashville, Tennessee 37208 USA

**ABSTRACT** We have examined the effect of 1-palmitoyl-2-(10-pyrenyl)decanoyl-*sn*-glycerol-3-phosphatidylcholine (Pyr-PC) concentration on the ratio of excimer fluorescence to monomer fluorescence (E/M) in L- $\alpha$ -dimyristoylphosphatidylcholine (DMPC) multilamellar vesicles at 30°C, with special attention focussed on the smoothness of the curve. We observed a series of dips, in addition to kinks, in the plot of E/M versus the mole fraction of Pyr-PC ( $X_{\text{PyrPC}}$ ). The observation of dips is a new finding, perhaps unique for Pyr-PC in DMPC since only kinks were observed for Pyr-PC in L- $\alpha$ -dipalmitoylphosphatidylcholine (DPPC) and in egg yolk phosphatidylcholine (egg-PC) (Somerharju et al., 1985. *Biochemistry*, 24: 2773–2781). The dips/kinks observed here are distributed according to a well defined pattern reflecting a lateral order in the membrane, and distributed symmetrically with respect to 50 mol% Pyr-PC. Some of the dips appear at specific concentrations ( $Y_{\text{PyrPC}}$ ) according to the hexagonal super-lattice model proposed by Virtanen et al. (1988. *J. Mol. Electr.* 4: 233–236). However, the observations of dips at  $X_{\text{PyrPC}} > 66.7$  mol% and the kink at 33.3 mol% cannot be interpreted by the model of Virtanen et al. (1988). These surprising results can be understood by virtue of an extended hexagonal super-lattice model, in which we have proposed that if the pyrene-containing acyl chains are regularly distributed as a hexagonal super-lattice in the DMPC matrix at a specific concentration  $Y_{\text{PyrPC}}$ , then the acyl chains of DMPC can form a regularly distributed hexagonal super-lattice in the membrane at a critical concentration ( $1 - Y_{\text{PyrPC}}$ ). The excellent agreement between the calculated and the observed dip/kink positions, except for the dip at 74 mol% and the kink at 40 mol%, provides most compelling evidence that lipids are regularly distributed into hexagonal super-lattices in Pyr-PC/DMPC mixtures at specific concentrations. The physical nature of the dips not only gives us a better understanding of lipid lateral organization in membranes but also will lead to new theoretical considerations and experimental designs for exploring the relationship between lipid regular distribution and membrane functions.

## INTRODUCTION

Lateral distribution of lipids in membranes is an important, but not well understood, phenomenon (for reviews, see Jain, 1983; Thompson and Tillack, 1985). The components of binary mixtures of lipids can be either phase separated, randomly distributed, or regularly distributed (Von Dreele, 1978). Information on lipid lateral distribution can be deduced from freeze-etch electron microscopy (e.g., Tillack et al., 1982; Thompson et al., 1985), fluorescence microscopy (e.g., Haverstick and Glaser, 1987; Rodgers and Glaser, 1991), calorimetry (e.g., Mabrey et al., 1978; Melchior, 1986), spin labels (e.g., Berclaz and McConnell, 1981), the thiolate-disulfide interchange method (Krisovitch and Regen, 1991), and computer simulations (e.g., Jan et al., 1984).

The fluorescence of pyrene-labeled phospholipids has also been used to determine lipid lateral distribution. The abrupt change in the ratio of the excimer to monomer fluorescence intensity (E/M) of 1-palmitoyl-2-(10-

pyrenyl)decanoyl)-*sn*-glycerol-3-phosphatidylcholine (Pyr-PC) has been used to monitor the temperature-induced changes in lipid lateral distribution (Galla and Hartmann, 1980; Jones and Lentz, 1986). Using oxygen quenching to determine the excimer formation constant, Chong and Thompson (1985) showed that liposomes composed of Pyr-PC and 1-palmitoyl-2-oleoyl-L- $\alpha$ -phosphatidylcholine (POPC) form a randomly mixed liquid-crystalline system in the temperature range of 15–55°C. Using both E/M and the phase/modulation data, Hresko et al. (1986) demonstrated that Pyr-PC is randomly distributed in both L- $\alpha$ -dimyristoylphosphatidylcholine (DMPC) and L- $\alpha$ -dipalmitoylphosphatidylcholine (DPPC) at temperatures outside the phase transition regions. Roseman and Thompson (1980) suggested, based on passive phospholipid transfer experiments, that Pyr-PC is randomly distributed in the DMPC matrix at  $T > T_m$  of DMPC, where  $T_m$  stands for the main phase transition temperature.

In addition to random distribution and domain formation, Pyr-PC has also been suggested to be regularly distributed in lipid membranes. A regular distribution is a lateral organization where the guest molecules (e.g., Pyr-PC) are maximally separated in the lipid matrix (e.g., DMPC) (Von Dreele, 1978). As shown by Somerharju et al. (1985), the plots of E/M versus the mole fraction of Pyr-PC,  $X_{\text{PyrPC}}$ , in egg yolk phosphatidylcholine (egg-PC) and in DPPC are not smooth; the plots have several linear regions separated by kinks. In a later

Address correspondence to Dr. Chong.

**Abbreviations used:** DMPC, L- $\alpha$ -dimyristoylphosphatidylcholine; DPPC, L- $\alpha$ -dipalmitoylphosphatidylcholine; egg-PC, egg yolk phosphatidylcholine; POPC, 1-palmitoyl-2-oleoyl-L- $\alpha$ -phosphatidylcholine; Pyr-PC, 1-palmitoyl-2-(10-pyrenyl)decanoyl-*sn*-glycerol-3-phosphatidylcholine;  $T_m$ , main phase transition temperature;  $X_{\text{PyrPC}}$ , mole fraction of Pyr-PC in DMPC;  $Y_{\text{PyrPC}}$ , critical mole fraction of Pyr-PC at which the acyl chains of DMPC form regularly distributed hexagonal super-lattices;  $Y_{\text{PyrPC}}$ , critical mole fraction of Pyr-PC at which the acyl chains containing the pyrene moiety form regularly distributed hexagonal super-lattices.

study of Pyr-PC in DPPC Langmuir-Blodgett films. Kinnunen et al. (1987) observed similar kinks in the E/M vs.  $X_{\text{PyrPC}}$  curve. A theory has been established by Virtanen et al. (1988) to determine the critical concentrations at which the kinks may be observed. In essence, the theory states that the kink is a result of regular distribution of Pyr-PC into a hexagonal super-lattice (Somerharju et al., 1985; Virtanen et al., 1988). The concept of regular distribution has been subsequently used to describe the lateral organization of cytochrome *c* in liposomes (Mustonen et al., 1987). By using a three-state model and the global analysis of the steady-state and phase-modulation fluorescence data, Sugar et al. (1991*b*) have recently shown that the lateral distribution parameter  $w$  (Sugar et al., 1991*a, b*) is negatively deviated from ideal mixing, which implies that Pyr-PC tends to be surrounded by DMPC molecules. It was then concluded that Pyr-PC molecules form regular rather than completely random distributions in the DMPC/Pyr-PC binary mixture. The new approach used by Sugar et al. (1991*a, b*) has dealt with the inadequacy of the two-state photophysical model constructed by Birks et al. (1963). In this regard, the conclusion of Sugar et al. (1991*b*) is significant; yet, whether the regular distribution is in the form of hexagonal super lattice remains unspecified.

In this study, we have examined the effect of Pyr-PC concentration on the E/M value in DMPC multilamellar vesicles, with special attention focused on the smoothness of the curve. We observed a series of dips, in addition to kinks, in the E/M vs.  $X_{\text{PyrPC}}$  curve at  $T > T_m$  of DMPC. These dips and kinks are found at specific concentrations of Pyr-PC and are distributed over a wide range of concentrations (0–100 mol%). This finding echoes the previous observation of kinks for Pyr-PC in DPPC and in egg-PC (Somerharju et al., 1985; Kinnunen et al., 1987) and provides strong supporting evidence for regular distribution of Pyr-PC in DMPC vesicles (Sugar et al., 1991*b*). Most importantly, the physical nature of dips gives us a better understanding of lipid lateral organization in membranes, which will lead to new theoretical considerations and experimental designs for exploring the relationship between lipid regular distribution and membrane functions.

## MATERIALS AND METHODS

### Materials

Pyr-PC was obtained from Molecular Probes (Eugene, OR) and was purified by high performance liquid chromatography with a C-18 reverse-phase column ( $3.9 \times 150$  mm,  $\mu$ -Bondapak; Millipore, Marlborough, MA) using methanol/acetonitrile (67:33, vol/vol) as the mobile phase. DPPC and DMPC were purchased from Avanti Polar Lipids (Alachua, FL) and used as such. The concentration of Pyr-PC was determined using an extinction coefficient at 342 nm equal to  $42,000 \text{ M}^{-1} \text{ cm}^{-1}$  (in methanol). The phospholipid concentration was determined as inorganic phosphate by the method of Bartlett (1959).

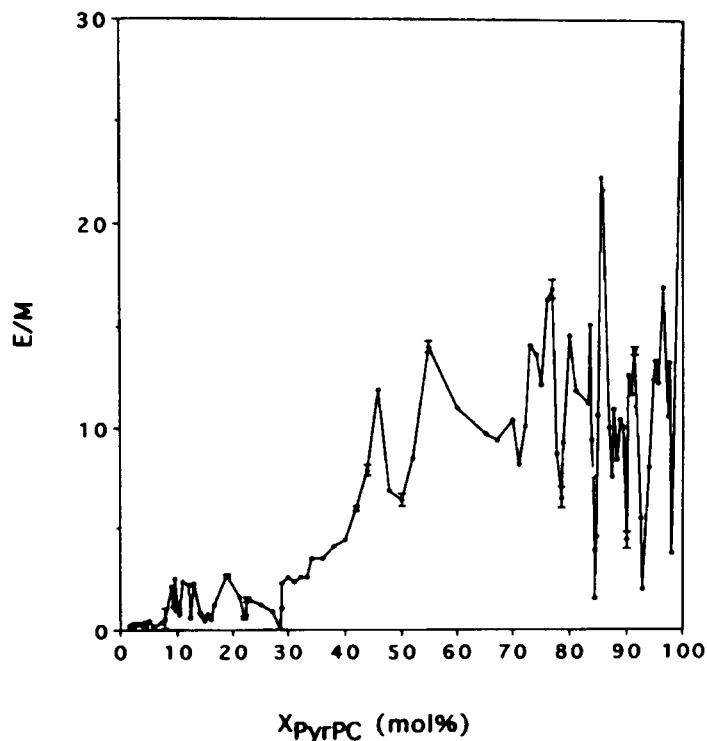


FIGURE 1 Concentration dependence of E/M for Pyr-PC in DMPC multilamellar vesicles at 30°C. The typical error bars are indicated, which represent the errors resulting from three to four measurements of the same sample preparation; the same situation applies to the data shown in Figs. 2–4.

### Preparation of liposomes

Pyr-PC and DMPC or DPPC were co-mixed in methanol. The mixtures were dried under vacuum overnight and then suspended in 50 mM KCl,  $10^{-4}$  M EDTA, and 10 mM Tris at pH 7.5. The dispersion was vortexed for 2 min at  $T > T_m$ . The samples were cooled to 4°C for 30 min and then placed at 38°C for 30 min. This cooling/heating cycle was repeated two more times. Finally, the samples were stored at 4°C overnight before fluorescence measurements. The concentration of lipids used for fluorescence measurements ranged from  $2 \times 10^{-7}$  to  $1 \times 10^{-6}$  M. The size of vesicles does not seem to change significantly with the Pyr-PC concentration, as revealed by the light scattering data (data not shown) obtained by a Coulter particle size analyzer (N4MD; Coulter).

### Fluorescence measurements

Fluorescence intensity measurements were made with an SLM DMX-1000 fluorometer (SLM Instruments, Urbana, IL). Samples were excited at 343 nm with 2-nm bandpass. The emission was observed through a monochromator with 4-nm bandpass. The ratio of excimer fluorescence (E) to monomer fluorescence (M) was determined using the intensities at 474 and 378 nm, respectively. All samples, unless otherwise specified, were measured within 36 h after preparation.

## RESULTS AND DISCUSSION

Fig. 1 shows the concentration dependence of E/M for Pyr-PC in DMPC multilamellar vesicles at 30°C. It is noticed that the curve is not smooth, as the cases of Pyr-PC in egg-PC and in DPPC observed by Somerharju et al. (1985) and by Kinnunen et al. (1987). In contrast to

their results, we show in the plot (Fig. 1) a number of dips, in addition to kinks. For example, the E/M decreases from 12 to 6.5 as the concentration of Pyr-PC changes from 48 to 50 mol% and then the E/M increases to 8.5 at 52 mol% Pyr-PC and 14 at 57 mol%. This reverse of the sign of the slope forms a dip at 50 mol%. A kink, on the other hand, is defined as the point in the curve where the slope undergoes a sudden change in magnitude, but not the sign. By this definition, a kink is found at 33.3 mol%, for instance. The dips are more clearly observable than the kinks. The observation of dips is a new finding, which may be unique for DMPC/Pyr-PC mixtures. Recall that only kinks, instead of dips, were observed for Pyr-PC in DPPC and in egg-PC (Sommerharju et al., 1985; Kinnunen et al., 1987). Air oxygen was found to have little effect (data not shown) on our results as the dips persist after the samples were flushed with nitrogen. The data pertaining to the dips were first thought to be scattered data due to experimental errors. After being able to reproduce the dips from several independent preparations (illustrated in Fig. 3), we now believe that the dips are real and they appear according to a well defined pattern reflecting a lateral order in the membrane (discussed later). This complicated shape was not realized in our previous studies of Pyr-PC in DMPC (Sugar and Chong, 1989; Sugar et al., 1991a) because fewer concentrations were measured in those studies.

Figs. 2–4 show the enlarged plots of E/M vs.  $X_{\text{PyrPC}}$  in different concentration regions. The concentrations at which the dips and kinks are observed are listed in Tables 1 and 2 (in parentheses). The observed dips shown in Table 1 can be understood in terms of the regular distribution model proposed by Virtanen et al. (1988). Their model proposes that (a) the acyl chains of the phospholipids form a hexagonal host lattice, (b) Pyr-PC chains are guest elements, which cause steric perturbation in the host lattice, and (c) the guest elements tend to be maximally separated in order to minimize the total free energy. According to Ruocco and Shipley (1982), the acyl chains of phospholipids can be arranged into a quasi two-dimensional hexagonal lattice, as illustrated in Fig. 5 A, in which the dark circles are the acyl chains containing the pyrene moiety and the open circles represent the unlabeled acyl chains. For a given acyl chain, its position can be described by two coordinates once the origin and the principal coordinates have been defined. Thus, the lateral position of a dark circle in Fig. 5 A can be described by a coordinate  $(n_a, n_b)$ , whereas  $n_a$  and  $n_b$  are the number of translational steps in the lattice along the two principal axes  $a$  and  $b$ , respectively. In the regular distribution, Pyr-PC molecules may establish a hexagonal "super-lattice" within the host lattice. Fig. 5 A illustrates such a super-lattice for  $n_a = 1$  and  $n_b = 1$  (see the lattice connected by the solid lines). The critical Pyr-PC mole fraction,  $Y_{\text{PyrPC}}(n_a, n_b)$ , for the pyrene-containing acyl chains to form the regularly distributed hexagonal super-

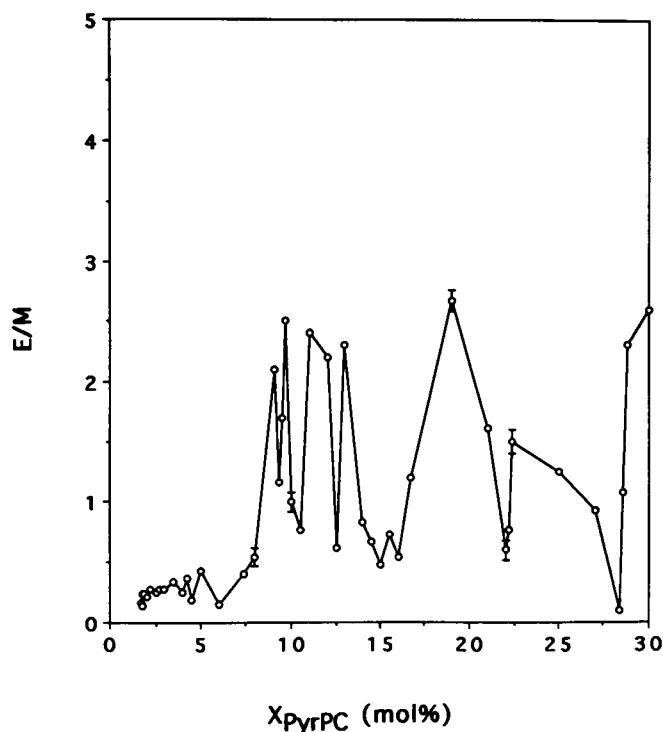


FIGURE 2 Enlarged plot of E/M vs.  $X_{\text{PyrPC}}$  in the Pyr-PC concentration range 0–30 mol%. These 42 points were derived from a single experiment with all these 42 samples prepared at the same time and having the same thermal history.

lattices can be calculated by the equation (Kinnunen et al., 1987; Virtanen et al., 1988)

$$Y_{\text{PyrPC}}(n_a, n_b) = 2/(n_a^2 + n_a n_b + n_b^2). \quad (1)$$

The calculated  $Y_{\text{PyrPC}}(n_a, n_b)$  values are listed in Table 1. All the observed dips/kinks shown in Table 1, except for the kink at 40 mol% (discussed later), are found to occur near the calculated  $Y_{\text{PyrPC}}(n_a, n_b)$  values. This suggests that the dips and kinks can be attributed to the formation of regularly distributed Pyr-PC super-lattices in the DMPC matrix, as modeled by Virtanen et al. (1988).

The surprising results are that we observed dips at  $X_{\text{PyrPC}} > 66.7$  mol% and a kink at 33.3 mol%. According to Eq. 1, the  $Y_{\text{PyrPC}}(n_a, n_b)$  value cannot exceed 66.7 mol% and there should not be a kink at 33.3 mol%. The dips observed at  $X_{\text{PyrPC}} > 66.7$  mol% and the kink observed at 33.3 mol% can be understood as follows. Assume that Pyr-PC and DMPC fit equally well into a hexagonal lattice. Then, the acyl chains of DMPC should also adopt a regularly distributed hexagonal super-lattice in the Pyr-PC matrix at specific concentrations. These specific concentrations can be calculated based on the idea that if Pyr-PC is regularly distributed as a super-lattice in the DMPC matrix at  $Y_{\text{PyrPC}}$  (e.g., 22.2 mol% Pyr-PC), then DMPC should be regularly distributed as a super-lattice in the Pyr-PC matrix at  $(1 - Y_{\text{PyrPC}})$  (e.g., 77.8 mol% Pyr-PC). Thus, the critical Pyr-PC mole frac-

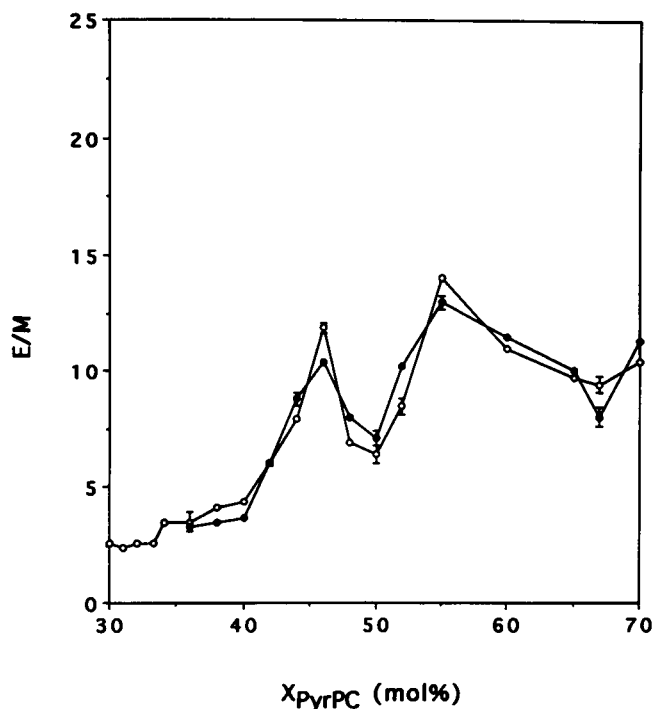


FIGURE 3 Enlarged plot of  $E/M$  vs.  $X_{\text{PyrPC}}$  in the concentration range of 30–70 mol% Pyr-PC with two different runs (—○— and —●—) superimposed on the same graph. In each run, all the points were derived from a single experiment with all the samples prepared at the same time and having the same sample history. This figure illustrates the good reproducibility of the dips and the dip positions. The variations in the absolute values of  $E/M$  at a given Pyr-PC concentration between different runs are not significant since the  $E/M$  value of Pyr-PC in DMPC is sensitive to the sample history and since it is almost impossible to reproduce the exact sample history between two different runs. For the sake of identifying the dips, only the curves of one run are presented in Figs. 1, 2, and 4.

tion,  $Y'_{\text{PyrPC}}(m_a, m_b)$ , at which the acyl chains of DMPC arrange into regularly distributed hexagonal super-lattices, can be expressed as:

$$Y'_{\text{PyrPC}}(m_a, m_b) = 1 - (2/(m_a^2 + m_a m_b + m_b^2)), \quad (2)$$

and the relationship between  $Y_{\text{PyrPC}}$  and  $Y'_{\text{PyrPC}}$  is given by:

$$Y'_{\text{PyrPC}}(m_a, m_b) = 1 - Y_{\text{PyrPC}}(n_a, n_b), \quad (3)$$

where  $a$  and  $b$  are the principal axes for the DMPC hexagonal super-lattice, and  $m_a$  and  $m_b$  are the projections along the axis  $a$  and  $b$ , respectively, for an acyl chain of DMPC (open circles) in the super-lattice (Fig. 5 B). Fig. 5 B illustrates a DMPC hexagonal super-lattice (open circles connected with lines) for the situation of  $m_a = 1$  and  $m_b = 1$  (i.e., 33.3 mol% Pyr-PC). The shaded circles in Fig. 5 B represent either the pyrene-containing acyl chains or those unlabeled acyl chains which do not participate in the super-lattice. The calculated  $Y'_{\text{PyrPC}}$  values are listed in Table 2, along with the concentrations where the dips/kinks are observed. There is a good agreement

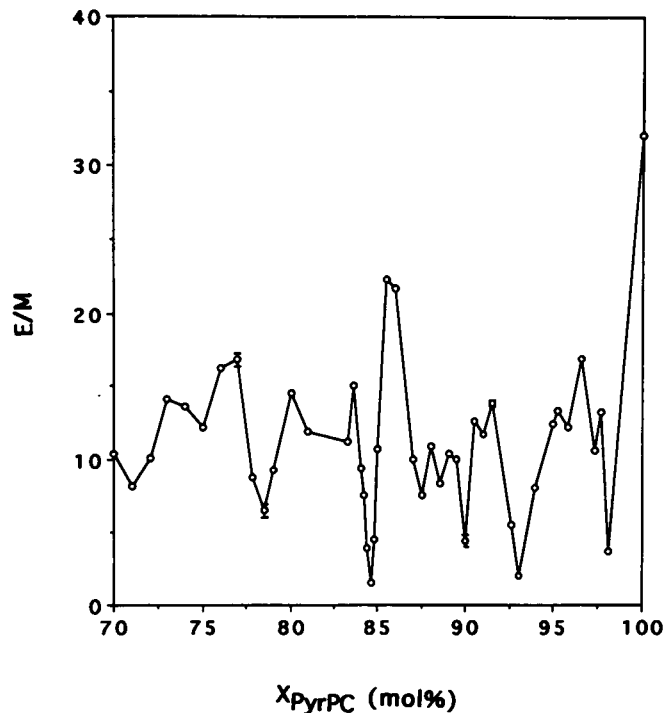


FIGURE 4 Enlarged plot of  $E/M$  vs.  $X_{\text{PyrPC}}$  in the concentration range of 70–100 mol% Pyr-PC. All the data points were derived from a single experiment with all these 44 samples prepared at the same time and having the same thermal history.

between the calculated and the observed dip positions, except for the dip at 74 mol% (discussed later). For example, when  $Y'_{\text{PyrPC}} = 77.8$  mol%, we expect the acyl chains

TABLE 1 Comparison between the observed dips/kinks and theoretically predicted critical Pyr-PC concentrations,  $Y_{\text{PyrPC}}$ , for the formation of the regularly distributed Pyr-PC super-lattices in the DMPC matrix

	$n_a$						
	0	1	2	3	4	5	6
1		66.7 (66.7)					
2	50.0 (50.0)	28.6 (26.0)	16.7 (16.0)				
3	22.2 (22.0)	15.4 (15.0)	10.5 (10.5)	7.4 (7.4)			
4	12.5 (12.5)	9.5 (9.4)	7.1	5.4	4.2 (4.5)		
$n_b$ 5	8.0	6.5	5.1	4.1 (4.0)	3.3	2.7	
6	5.6	4.7	3.8	3.2	2.6	2.2	1.9
7	4.1	3.5	3.0 (3.0)	2.5	2.2	1.8 (1.8)	1.6
8	3.1	2.7 (2.7)	2.4	2.1	1.8 (1.8)	1.6	1.4
9	2.5 (2.5)	2.2	1.94	1.7 (1.7)	1.5	1.3	1.2

The numbers in parentheses are the Pyr-PC concentrations where the dips were observed.

TABLE 2 Comparison between the observed dips/kinks and theoretically predicted critical Pyr-PC concentrations,  $Y'_{\text{PyrPC}}$ , at which the acyl chains of DMPC form regularly distributed hexagonal super-lattices in the membrane

	$m_a$						
	0	1	2	3	4	5	6
$m_b$	1	33.3 (33.3)*					
	2	50.0 (50.0)	71.4 (71.0)	83.3 (83.3)			
	3	77.8 (78.0)	84.6 (84.6)	89.5 (89.5)	92.6 (93.0)		
	4	87.5 (87.5)	90.5 (90.0)	92.9 (93.0)	94.6 (95.8)	95.8 (95.8)	
	5	92.0 (91.0)	93.5	94.9	95.9 (95.8)	96.7 (97.3)	97.3 (97.3)
	6	94.4	95.3	96.2	96.8	97.4	97.8 (98.2)
	7	95.9	96.5	97	97.5	97.8	98.2
	8	96.9	97.3	97.6	97.9	98.2	98.4
	9	97.5	97.8	98.1	98.3	98.5	98.7

The numbers in parentheses are the Pyr-PC concentrations where the dips or kinks\* were observed.

of DMPC regularly distributed into a hexagonal super-lattice, according to Eq. 2. Indeed, at 78 mol% Pyr-PC, we observed a dip (Fig. 4 and Table 2). Using Eq. 2, we can also explain why a kink at 33.3 mol% is observed (Fig. 3). According to Eq. 2, a regularly distributed super-lattice for the acyl chains of DMPC should appear at 33.3 mol% Pyr-PC (i.e., a lattice with  $m_a = 1$  and  $m_b = 1$ ) (Table 2). Thus, the kink observed at 33.3 mol% Pyr-PC is not by accident; it is likely to result from a regular distribution with  $m_a = 1$  and  $m_b = 1$ , as illustrated in Fig. 5 B. In summary, the observations of dips at  $X_{\text{PyrPC}} > 66.7$  mol% and the kink at 33.3 mol% are a critical finding, which greatly substantiates the idea that lipids are regularly distributed into hexagonal super-lattices in Pyr-PC/DMPC mixtures at specific concentrations.

For the purpose of comparison between the theoretical and the observed values, the dips/kinks in the intermediate concentration region (25–75 mol%) turn out to be more useful than those in the low and high concentration regions. Fig. 6 shows the distribution of the theoretical dips/kinks as a function of  $X_{\text{PyrPC}}$ . It is found that the distribution is symmetric  $\sim 50$  mol% line, with a much higher frequency of appearance at both low and high concentration ends. In this intermediate concentration region, the dips/kinks are less closely packed. Hence, the positions of the dips/kinks in this region can be less ambiguously determined. The excellent agreement between the positions of the dips/kinks (except for the dip at 74 mol% and the kink at 40 mol%, Figs. 3 and 4) and the calculated  $Y_{\text{PyrPC}}$  or  $Y'_{\text{PyrPC}}$  values in the intermediate concentration region (Tables 1 and 2) provides the most compelling evidence that the dips/kinks do not appear randomly and that the appearance of kinks/dips is a re-

sult of lipid regular distribution into hexagonal super-lattices.

It should be mentioned that samples stored for 2 mo at 4°C still exhibited the dips/kinks at the specific concentrations (data not shown). This indicates that the dips

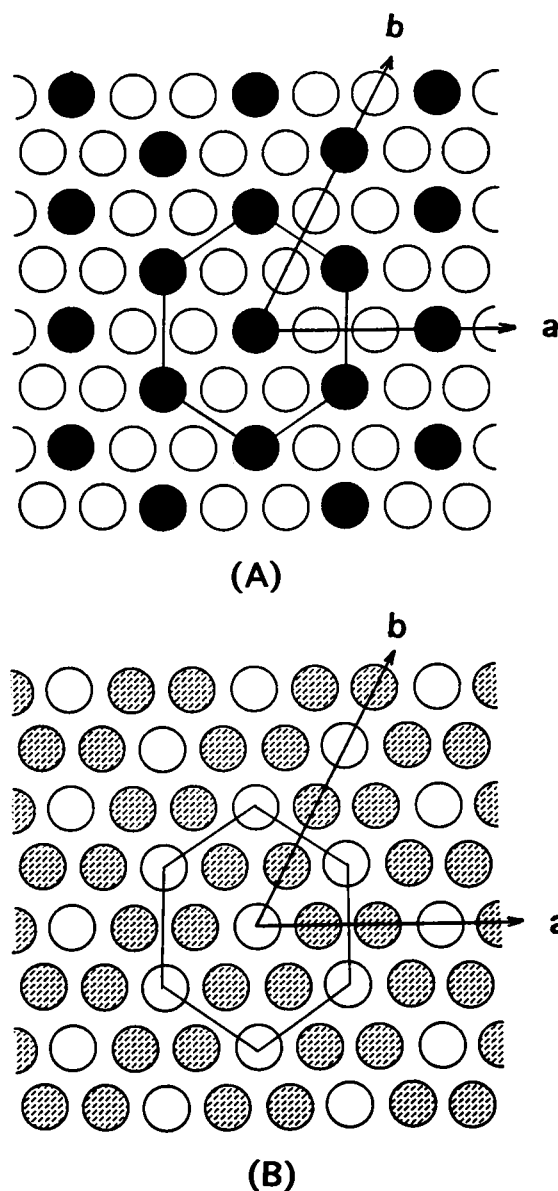


FIGURE 5 (A) Schematic diagram for Pyr-PC regularly distributed into a hexagonal super-lattice (see the lattice connected by the lines) with  $m_a = 1$  and  $m_b = 1$  in the Pyr-PC/DMPC mixture (66.7 mol% Pyr-PC). The dark circles represent the acyl chains containing pyrene moiety and the open circles represent the unlabeled acyl chains. The symbols are defined in the text. This diagram follows the model presented by Virtanen et al. (1988). (B) Schematic diagram showing the acyl chains of DMPC regularly distributed into a hexagonal super-lattice (see the lattice connected by the lines) with  $m_a = 1$  and  $m_b = 1$  in the Pyr-PC/DMPC mixture (33.3 mol% Pyr-PC). The open circles represent the acyl chains of DMPC involved in the super-lattice. The dashed circles represent either the pyrene-containing acyl chains or those DMPC acyl chains which do not participate in the super-lattice. The symbols are defined in the text.

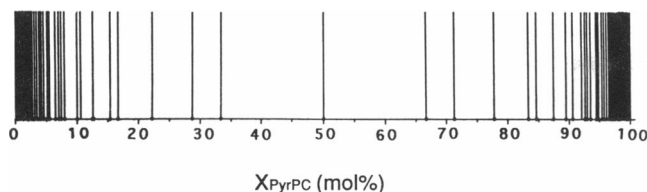


FIGURE 6 The distribution of the predicted dips (using Eqs. 1 and 2) over the concentration range of 0–100 mol%.

appear both within 36 h of sample preparation (Tables 1 and 2) and at equilibrium via long term incubation. The implication is that the regular distribution is a long lived, not a transient, phenomenon.

Because the dips observed at 74 mol% Pyr-PC (Fig. 4) and the kink at 40 mol% (Fig. 3) are not those theoretically predicted for hexagonal super-lattice arrangements, these two points require some comments. The dip at 74 mol% and the kink at 40 mol% may result from two or more hexagonal super-lattices. For example, the dip at 74 mol% may reflect a complex lateral organization composed of two hexagonal super-lattices: 20% of Pyr-PC molecules having the ( $m_a = 1$ ,  $m_b = 1$ ) lattice and 80% having the ( $m_a = 0$ ,  $m_b = 3$ ) lattice; or, 10% of Pyr-PC in the ( $m_a = 1$ ,  $m_b = 1$ ) lattice plus 90% of Pyr-PC in the ( $m_a = 2$ ,  $m_b = 2$ ) lattices. These putative complex lateral organizations may arise from compositional heterogeneity in lipid vesicles. It is likely that, in certain sample preparations, not all the vesicles contain the same amount of Pyr-PC. It is also likely that there exists some heterogeneity between super lattices in the inner and outer monolayers.

Our present experimental data show dips/kinks over a wide range of  $X_{\text{PyrPC}}$ . In the studies of Pyr-PC in DPPC and Pyr-PC in Egg-PC liposomes (Somerharju et al., 1985), the Pyr-PC concentration was limited to 10 mol%; and, only two kinks were observed (3.8 mol% and 6.8 mol% for Pyr-PC in DPPC; 5.0 mol% and 10.0 mol% for Pyr-PC in egg-PC). In the study of monolayers of DPPC (Kinnunen et al., 1987), the Pyr-PC concentration was extended to 67 mol%; yet, only 5 kinks were seen (at 66, 28, 16.5, 7.4, and 3.8 mol% Pyr-PC). Our present data cover the concentration of Pyr-PC up to 100 mol%. We found previously unnoticed dips, especially the dips at high  $X_{\text{PyrPC}}$ . Although our present data show more dips/kinks, still, not all the theoretically predicted  $Y_{\text{PyrPC}}$  or  $Y'_{\text{PyrPC}}$  values readily display kinks or dips. This may be due to the experimental difficulties in preparing samples with minute differences in concentrations. Consequently, some of the theoretically predicted critical points, particularly those in the low and high concentration regions, cannot be resolved. As an example, a large number of critical concentrations are predicted in the region of 96–99 mol% (Table 2). Instead of seeing numerous lines, we observed a single dip in the neighborhood

of 97 mol%. This dip is likely to be a composite of many different dips closely packed in the region.

The presence of dips/kinks in the plot of E/M vs.  $X_{\text{PyrPC}}$  (Fig. 1) suggests that the E/M value is not always proportional to the concentration of Pyr-PC. Although the deviation from linearity at high Pyr-PC concentrations was noticed before (Sugar and Chong, 1989), it has been thought for some time that at low concentrations (e.g., < 5 mol% Pyr-PC), the relationship between E/M and  $X_{\text{PyrPC}}$  is linear. Apparently, this is not correct, because many kinks/dips are involved in the low concentration region (Fig. 2 and Table 1).

The presence of dips/kinks also suggests that the formation of excimer is not only determined by the lateral diffusion of Pyr-PC, but also by its lateral distribution. Our experiment was carried out at 30°C, which is above the phase transition temperatures of both Pyr-PC and DMPC. At 30°C, the Pyr-PC/DMPC membrane is in the fluid liquid crystalline state. In this rather fluid environment, the lateral diffusion of Pyr-PC brings about the collision between the ground state monomer and the excited state monomer, leading to the formation of excimer. As such, the E/M of Pyr-PC is expected to increase as  $X_{\text{PyrPC}}$  increases, assuming that lateral diffusion is the only determinant for excimer formation. However, we observed that the E/M decreases with  $X_{\text{PyrPC}}$  when  $X_{\text{PyrPC}}$  approaches  $Y_{\text{PyrPC}}$  or  $Y'_{\text{PyrPC}}$  (Fig. 1). This implies that factors other than lateral diffusion need to be considered for the formation of excimers. Note that similar conclusions have been made previously by others. Blackwell et al. (1986) suggested that pyrene excimer formation in membranes originates from pyrene aggregates, rather than diffusion. Sugar et al. (1991b) proposed a three-state model and pointed out the importance of pyrene ring orientations between neighboring molecules in the formation of excimers. Kinnunen et al. (1987) suggested that the kinks in the plot of E/M vs.  $X_{\text{PyrPC}}$  are not due to lateral diffusion, but due to long range lattice coherence. Here we provide a somewhat different view. As discussed before, at the dip concentrations, the guest molecules are regularly distributed into a hexagonal super-lattice, and they are maximally separated in order to minimize the total free energy (Virtanen et al., 1988). Note that, in binary mixtures, when the molecules of the first component are maximally separated, the molecules of the second component are also maximally separated. When the intermolecular distance between Pyr-PC is maximized, the chances for excimer formation are reduced. This explains why the E/M drops at  $Y_{\text{PyrPC}}$  or at  $Y'_{\text{PyrPC}}$ . At concentrations slightly below  $Y_{\text{PyrPC}}$  or  $Y'_{\text{PyrPC}}$ , the lateral organization of lipid molecules drifts toward the hexagonal super-lattice pattern. At concentrations slightly above  $Y_{\text{PyrPC}}$  or  $Y'_{\text{PyrPC}}$ , the lateral distribution moves away from the hexagonal super-lattice arrangement. It is this concentration-dependent balance between the energy minimization and

the entropy-driven randomization that creates dips. In Pyr-PC/DPPC and Pyr-PC/egg-PC, only kinks were reported (Somerharju et al., 1985; Kinnunen et al., 1987). The inability to observe dips in Pyr-PC/DPPC and in Pyr-PC/egg-PC may be related to the differences in the interaction free energy between lipid molecules. The interaction free energy between Pyr-PC and DMPC must be different from that between Pyr-PC and DPPC. Although, at  $Y_{\text{PyrPC}}$ , Pyr-PC molecules are regularly distributed into hexagonal super-lattices in both DMPC (this study) and DPPC (Somerharju et al., 1985), the energy minimization due to this special lateral organization is likely to be different in different systems. Perhaps, the energy minimization due to the hexagonal super-lattice regular distribution is to a lesser extent in the case of Pyr-PC in DPPC, as compared with Pyr-PC in DMPC; thus, only kinks were observed in the Pyr-PC/DPPC mixtures.

It should be mentioned that the presence of a lateral order (such as the hexagonal super-lattice depicted in Fig. 5) in the liquid crystalline state of DMPC does not lead to  $E/M = 0$ . At  $Y'_{\text{PyrPC}}$  (except for 33.3 mol% Pyr-PC), the acyl chains of DMPC form a regularly distributed hexagonal super-lattice whereas the Pyr-PC molecules may organize into domains. This automatically explains why  $E/M$  does not go to zero at  $Y'_{\text{PyrPC}}$ . At  $Y_{\text{PyrPC}}$ , the pyrene-containing acyl chains are maximally separated. If the lateral diffusion of Pyr-PC is fast, compared with the emission rate of Pyr-PC fluorescence, then  $E/M$  will not go to zero. The lateral diffusion coefficient of Pyr-PC in DMPC at 30°C has been determined to be in the range of 19–24  $\mu\text{m}^2/\text{s}$  (Galla et al., 1979; Sassaroli et al., 1990; Sugar et al., 1991b). Using a molecular area at the bilayer surface of 38.9  $\text{\AA}^2$  for both DMPC (Pearson and Pascher, 1979) and Pyr-PC, one can calculate that Pyr-PC traverses about only one lipid molecule during the fluorescence lifetime ( $\tau$ ) of Pyr-PC (assuming that  $\tau = 20$  ns). This cannot explain why the  $E/M$  value does not go to zero at  $Y_{\text{PyrPC}}$ . The nonzero  $E/M$  value at  $Y_{\text{PyrPC}}$  may be explained by the existence of imperfect hexagonal super-lattices (in contrast to the perfect hexagonal super-lattice shown in Fig. 5) in some part of the membrane at  $Y_{\text{PyrPC}}$ . The imperfect super-lattice, probably arising from impurity or changes in membrane curvature, would allow a greater local lateral mobility (Vaz et al., 1985) for Pyr-PC molecules to form excimers. Alternatively, the nonzero  $E/M$  value can be explained by the concept of long range lattice coherence proposed by Kinnunen et al. (1987). This theory suggests that an excimer can be formed by quantum mechanical coupling of pyrene wave functions at a distance. The third possibility lies in the excimer formation between Pyr-PC molecules residing in the opposite leaflets of the bilayers. The acyl chains of DMPC are shorter than those in Pyr-PC, therefore, the pyrene moiety is likely to extend in part between the acyl chains of the opposing monolayers.

At the present time, we do not know the lateral distribution of lipids in the Pyr-PC/DMPC mixture at  $X_{\text{PyrPC}}$  between the dip points. This information may be obtained by considering a hexagonal super-lattice type of regular distribution at dip (or kink) concentrations in the Monte Carlo simulation (e.g., Sugar and Chong, 1989) or in the global analysis of E/M and the phase/modulation data of pyrene fluorescence (Sugar et al., 1991a, b).

The present observation that the dips/kinks appear according to Eqs. 1 and 2 is of fundamental importance in the field of membrane organization. Since the first observation of kinks by Somerharju et al. (1985), little has been done with regard to the physical basis and the functional role of lipid regular distribution, partly due to the rather limited data for kinks in the previous works (Somerharju et al., 1985; Kinnunen et al., 1987). Our present data show many dips, in addition to kinks, over a wide range of concentrations; and, almost all of the dips/kinks can be interpreted by the extended hexagonal super-lattice model proposed in this paper. Using the dips and the dip positions as the indices of lipid regular distribution, we will address a series of questions pertaining to the role of lipid regular distribution in membrane functions such as membrane fusion, lipid transfer, ligand (or drug) binding, and protein insertion. The lipid-mediated long range order may have important consequences for the function of biological membranes (Kinnunen, 1991).

We thank Dr. I. P. Sugar for his stimulating discussions, and Mr. Junwen Zeng and Ms. Lihua Wei for their technical assistance.

This work was supported by the U.S. Army Research Office, NSF (R11-8714805), and NIH (S06GM08037-20). This work was done during the tenure of an Established Investigator Award (to P. L.-G. Chong) from the American Heart Association and CIBA-GEIGY.

Received for publication 20 April 1992 and in final form 25 June 1992.

## REFERENCES

- Bartlett, G. R. 1959. Phosphorus assay in column chromatography. *J. Biol. Chem.* 234:466–468.
- Berclaz, T., and H. M. McConnell. 1981. Phase equilibria in binary mixtures of dimyristoylphosphatidylcholine and cardiolipin. *Biochemistry*. 20:6635–6640.
- Birks, J. B., D. J. Dyson, and I. H. Munro. 1963. Excimer fluorescence. II. Lifetime studies of pyrene solutions. *Proc. R. Soc. London, Ser. A.* 275:575–588.
- Blackwell, M. F., K. Gounaris, and J. Barber. 1986. Evidence that pyrene excimer formation in membranes is not diffusion-controlled. *Biochim. Biophys. Acta.* 858:221–234.
- Chong, P. L.-G., and T. E. Thompson. 1985. Oxygen quenching of pyrene-lipid fluorescence in phosphatidylcholine vesicles. A probe for membrane organization. *Biophys. J.* 47:613–621.
- Galla, H. J., and E. Hartmann. 1980. Excimer-forming lipids in membrane research. *Chem. Phys. Lipids.* 27:199–219.
- Galla, H. J., W. Hartmann, U. Theilen, and E. Sackmann. 1979. On

- two-dimensional passive random walk in lipid bilayers and fluid pathways in biomembranes. *J. Membr. Biol.* 48:215–236.
- Haverstick, D. M., and M. Glaser. 1987. Visualization of  $\text{Ca}^{2+}$ -induced phospholipid domains. *Proc. Natl. Acad. Sci. USA.* 84:4475–4479.
- Hresko, R. C., I. P. Sugar, Y. Barenholz, and T. E. Thompson. 1986. Lateral distribution of a pyrene-labeled phosphatidylcholine in phosphatidylcholine bilayers: fluorescence phase and modulation study. *Biochemistry.* 25:3813–3823.
- Jain, M. K. 1983. Nonrandom lateral organization in bilayers and biomembranes. In *Membrane Fluidity in Biology*. R. C. Aloia, editor. Vol. 1. Academic Press, New York. 1–37.
- Jan, N., T. Lookman, and D. A. Pink. 1984. On computer simulation methods used to study models of two-component lipid bilayers. *Biochemistry.* 23:3227–3231.
- Jones, M. E., and B. R. Lentz. 1986. Phospholipid lateral organization in synthetic membranes as monitored by pyrene-labeled phospholipids: effects of temperature and prothrombin fragment 1 binding. *Biochemistry.* 25:567–574.
- Kinnunen, P. K. J. 1991. On the principles of functional ordering in biological membranes. *Chem. Phys. Lipids.* 57:375–399.
- Kinnunen, P. K. J., A. Tulkki, H. Lemmetyinen, J. Paakkola, and A. Virtanen. 1987. Characteristics of excimer formation in Langmuir-Blodgett assemblies of 1-palmitoyl-2-pyrenedecanoylphosphatidylcholine and dipalmitoylphosphatidylcholine. *Chem. Phys. Lett.* 136:539–545.
- Krisovitch, S. M., and S. L. Regen. 1991. Nearest-neighbor recognition in phospholipid bilayers. Probing lateral organization at the molecular level. *J. Am. Chem. Soc.* 113:8175–8177.
- Mabrey, S., P. L. Mateo, and J. M. Sturtevant. 1978. High-sensitivity scanning calorimetric study of mixtures of cholesterol with dimyristoyl- and dipalmitoylphosphatidylcholines. *Biochemistry.* 17:2464–2468.
- Melchior, D. L. 1986. Lipid domains in fluid membranes: a quick-freeze differential scanning calorimetric study. *Science (Wash. DC).* 234:1577–1580.
- Mustonen, P., J. A. Virtanen, P. J. Somerharju, and P. K. J. Kinnunen. 1987. Binding of cytochrome c to liposomes as revealed by the quenching of fluorescence from pyrene-labeled phospholipids. *Biochemistry.* 26:2991–2997.
- Pearson, R. H., and I. Pascher. 1979. The molecular structure of lecithin dihydrate. *Nature (Lond.).* 281:499–501.
- Rodgers, W., and M. Glaser. 1991. Characterization of lipid domains in erythrocyte membranes. *Proc. Natl. Acad. Sci. USA.* 88:1364–1368.
- Roseman, M. A., and T. E. Thompson. 1980. Mechanism of the spontaneous transfer of phospholipids between bilayers. *Biochemistry.* 19:439–444.
- Ruocco, M. J., and G. G. Shipley. 1982. Characterization of the sub-transition of hydrated dipalmitoyl phosphocholine bilayers. Kinetics, hydration and structural studies. *Biochim. Biophys. Acta.* 691:309–320.
- Sassaroli, M., M. Vauhkonen, D. Perry, and J. Eisinger. 1990. Lateral diffusivity of lipid analogue excimeric probes in dimyristoylphosphatidylcholine bilayers. *Biophys. J.* 57:281–290.
- Somerharju, P. J., J. A. Virtanen, K. K. Eklund, P. Vainio, and P. K. J. Kinnunen. 1985. 1-Palmitoyl-2-pyrenedecanoyl glycerophospholipids as membrane probes: evidence for regular distribution in liquid-crystalline phosphatidylcholine bilayers. *Biochemistry.* 24:2773–2781.
- Sugar, I. P., and P. L.-G. Chong. 1989. Determination of the lateral distribution of lipid molecules in two-component membranes. Evaluation of pyrene fluorescence data. In *Biomedical Modelling and Simulation*. J. C. Baltzer and D. S. Levine, editors. Scientific Publishing Co. 73–78.
- Sugar, I. P., J. Zeng, M. Vauhkonen, P. Somerharju, and P. L.-G. Chong. 1991a. Use of Fourier transforms in the analysis of fluorescence data. 2. Fluorescence of pyrene-labeled phosphatidylcholine in lipid bilayer membranes. Test of the Birks model. *J. Phys. Chem.* 95:7516–7523.
- Sugar, I. P., J. Zeng, and P. L.-G. Chong. 1991b. Use of Fourier transforms in the analysis of fluorescence data. 3. Fluorescence of pyrene-labeled phosphatidylcholine in lipid bilayer membrane. A three-state model. *J. Phys. Chem.* 95:7524–7534.
- Tillack, T. W., M. Wong, A. Margareta, and T. E. Thompson. 1982. Organization of the glycosphingolipid asialo-GM1 in phosphatidylcholine bilayers. *Biochim. Biophys. Acta.* 691:261–273.
- Thompson, T. E., M. Allietta, M., R. E. Brown, M. C. Johnson, and T. W. Tillack. 1985. Organization of ganglioside GM1 in phosphatidylcholine bilayers. *Biochim. Biophys. Acta.* 817:229–237.
- Thompson, T. E., and T. W. Tillack. 1985. Organization of glycosphingolipids in bilayers and plasma membranes of mammalian cells. *Annu. Rev. Biophys. Chem.* 14:361–368.
- Vaz, W. L. C., R. M. Clegg, and D. Hallmann. 1985. Translational diffusion of lipids in liquid crystalline phase phosphatidylcholine multilayers. A comparison of experiment with theory. *Biochemistry.* 24:781–786.
- Virtanen, J. A., P. Somerharju, and P. K. J. Kinnunen. 1988. Prediction of patterns for the regular distribution of soluted guest molecules in liquid crystalline phospholipid membranes. *J. Mol. Elect.* 4:233–236.
- Von Dreelle, P. H. 1978. Estimation of lateral species separation from phase transitions in nonideal two-dimensional lipid mixtures. *Biochemistry.* 17:3939–3943.